Hamiltonian plasma-harmonic oscillator theory: Generalized depth profilometry of electronically continuously inhomogeneous semiconductors and the inverse problem

Alex Salnick[a] and Andreas Mandelis
Photothermal and Optoelectronic Diagnostics Laboratory, Department of Mechanical Engineering, University of Toronto, Toronto, Ontario M5S 3G8, Canada

(Received 28 May 1996; accepted for publication 2 August 1996)

The Hamilton–Jacobi formalism of the propagation of an electron-hole photoexcited plasma in continuously inhomogeneous semiconductors with arbitrary depth profiles in carrier diffusivity and/or minority-carrier lifetime is presented. The theoretical model is based on the variational formulation of the canonical Hamiltonian for the evolution of carrier plasmas and shows that propagating plasma waves can be formally described by a plasma-harmonic oscillator, thus generalizing existing theoretical treatments of photoexcited carrier diffusion in electronic solids. Simple analytical expressions for the free-carrier diffusion magnitude and phase frequency dependencies in the case of exponential carrier diffusivity and minority carrier lifetime profiles are obtained. The effect of continuously varying electronic properties on the surface plasma density magnitude and phase frequency behavior is demonstrated through computer simulations and very good quantitative agreement is obtained with photothermal radiometric data from an ion-implanted Si wafer allowing the reconstruction of the lifetime depth profile. © *1996 American Institute of Physics.* [S0021-8979(96)07821-8]

I. INTRODUCTION

In recent years, an increasing number of activities dealing with the photoacoustic and photothermal characterization of semiconductors is being reported in scientific journals. Several laser-based photothermal techniques have been developed to monitor photoexcited carrier kinetics and transport in semiconductors, the advantage over other, usually electrical, methods being that electronic effects can be monitored in a noncontacting and nondestructive manner.[1] Infrared photothermal radiometry (PTR),[2–4] photothermal beam deflection (PBD),[5,6] and photomodulated thermoreflectance (PMTR)[7] are the most frequently used techniques in these noncontact studies. Among the physical parameters of interest, the electronic transport properties of a semiconductor, namely, the carrier diffusivity (D_n), the minority carrier lifetime (τ), and the surface recombination velocity (s), have attracted great attention as the measurement of τ and D_n is useful in characterizing the quality of semiconductor materials and modeling semiconductor devices. These photothermal studies are based on the well known fact that the absorption of an intensity modulated or pulsed irradiation by semiconductors results in temperature and plasma density profiles whose temporal behavior is affected by the thermal and electrical transport characteristics of the material, thus allowing the main thermal and electronic transport parameters to be derived from the photothermal amplitude and phase (frequency domain) or time evolution (time domain) dependencies.[1,8]

The common characteristic feature of all previous theoretical and experimental photothermal studies of semiconductors is that only homogeneous or discontinuously inhomogeneous materials[9] (i.e., materials having a structure of subsurface layers of finite thickness) have been assumed. Correspondingly, both τ and D_n values have been usually referred to as the bulk or layer characteristics of a semiconductor. In spite of the fact that the possibility to use the plasma waves for depth profiling in semiconductors has been shown, at least in principle, for some time,[10] no experimental works or theoretical models have addressed the problem of τ and D_n profile reconstruction. Yet, such models are of special interest in the most important, and frequently more common, case of continuously inhomogeneous semiconductors.

The present article is the result of the realization that an electron-hole photoexcited plasma in an electronically active layer (e.g., a semiconductor substrate or thin surface layer device), when driven by a harmonically modulated irradiation and detected by a suitable detection (photothermal) technique, behaves like a carrier density diffusive wave,[9] and, therefore, it can be theoretically treated as a plasma-harmonic oscillator (PHO), using the Hamilton–Jacobi formalism of a classical mechanical harmonic oscillator.[11] As a consequence, a so far nonexistent solution to the pseudodiffusive-field plasma-wave problem for continuously inhomogeneous semiconductors with arbitrary τ and/or D_n depth profiles materializes as a generalized theory of free carrier diffusion in electronic solids. It is shown that the PHO approach allows the monitoring of the changes in photothermal signal frequency behavior due to various types of simulated inhomogeneities in a semiconductor induced by depth-dependent τ and D_n, and leads to a methodology for solving the inverse physical problem of the reconstruction of carrier recombination lifetime as a function of the depth coordinate in a semiconductor.

[a]Electronic mail: salnik@me.utoronto.ca

 0021-8979/96/80(9)/5278/11/$10.00

II. THEORETICAL MODEL

A. Canonical Hamiltonian formulation of the Hamilton–Jacobi PHO

The mathematical treatment of the problem is based on two physical conditions. First, the one-dimensional formulation of the carrier continuity equation is used in order to simplify the formalism, with the three-dimensional case constituting a straightforward extension of the fundamental concepts developed herein. Second, a strong optical absorption at the surface is assumed, and recombination to be only localized on the sample surface, thus neglecting the influence of a space charge region.

A semi-infinite semiconductor sample is considered, having a depth-dependent minority carrier lifetime $\tau(x)$ (s), carrier diffusivity $D_n(x)$ (cm^2/s), and constant surface recombination velocity s (cm/s), illuminated with a plane wave of monochromatic laser light. The laser light has angular modulation frequency ω (rad/s), flux Φ_0 (W/cm^2), photon energy $h\nu(J)$, and excitation efficiency equal to unity.

Considering only the ac solution for the photoexcited carrier density $n(x,t)$ of the form:

$$n(x,t)=N(x)e^{i\omega t}, \tag{1}$$

the carrier continuity equation can be written as

$$\frac{d}{dx}\left(D_n(x)\,\frac{dN(x)}{dx}\right)-\frac{N(x)}{\tau(x)}-i\omega N(x)=0, \tag{2}$$

with the boundary conditions:

$$D_n(x)\,\frac{dN(x)}{dx}\bigg|_{x=0}=-\frac{\Phi_0}{h\nu}+sN(0) \tag{3}$$

and

$$N(\infty)=0. \tag{4}$$

Using the variational formulation

$$\int_0^\infty\left[\frac{d}{dx}\left(D_n(x)\,\frac{dN(x)}{dx}\right)-\frac{1+i\omega\tau(x)}{\tau(x)}\,N(x)\right]\delta N dx=0, \tag{5}$$

and applying the boundary conditions we obtain

$$\delta\left\{N(0)(sN(0)-N_0)-\frac{1}{2}\int_0^\infty\left[D_n(x)\left(\frac{dN(x)}{dx}\right)^2+\frac{1+i\omega\tau(x)}{\tau(x)}\,N^2(x)\right]dx\right\}=0, \tag{6}$$

where $N_0=\Phi_0/h\upsilon(c/n)$. c/n is the speed of the propagation of optical radiation in a condensed medium of refractive index n.

Defining the Lagrangian function as

$$\mathscr{L}\equiv\frac{1}{2}\,D_n(x)\left(\frac{dN(x)}{dx}\right)^2+\frac{1}{2}\left(\frac{1+i\omega\tau(x)}{\tau(x)}\right)N^2(x), \tag{7}$$

and omitting the $N(0)[sN(0)-N_0]$ term here, which will be retrieved later from the field integration constants, yields the Hamiltonian

$$\mathscr{H}(x,N,p_n)=p_n(x)\,\frac{dN(x)}{dx}-\mathscr{L}=\frac{p_n^2(x)}{2D_n(x)}-\frac{1+i\omega\tau(x)}{\tau(x)}\,N^2(x), \tag{8}$$

with p_n the generalized momentum defined by

$$p_n(x)=\frac{\partial\mathscr{L}}{\partial\left(\frac{dN}{dx}\right)}=D_n(x)\,\frac{dN(x)}{dx}. \tag{9}$$

Equations (8) and (9) show that for the plasma-wave problem the generalized coordinate and momentum are the carrier concentration and flux, respectively, in the same manner as for the thermal wave the relevant parameters are the temperature and heat flux.[12] The Hamiltonian form is not appropriate, however, for use in the consideration of plasma wave dynamics, because it is an explicit function of the spatial coordinate (x). A canonical transformation is required, such that both coordinate and momentum will be constants of the motion.

Upon the introduction of two new variables

$$\zeta(x)=\int_0^x\left(\frac{1+i\omega\tau(y)}{i\omega\tau(y)D_n(y)}\right)^{1/2}dy \tag{10}$$

and

$$\alpha(x)=\left[D_n(x)\left(\frac{1+i\omega\tau(x)}{i\omega\tau(x)}\right)\right]^{1/4}N(x), \tag{11}$$

we obtain the PHO Hamiltonian

$$\mathscr{H}(p_n,\alpha)=\frac{1}{2}\,p_n^2-\frac{i\omega}{2}\,\alpha^2, \tag{12}$$

which is the analog of the classical canonical Hamiltonian function $H(p_n,\alpha)=p_n^2/2m+K\alpha^2/2$ with the following effective physical assignations of a harmonic oscillator:

$$\alpha=\left[D_n(x)\left(\frac{1+i\omega\tau(x)}{i\omega\tau(x)}\right)\right]^{1/4}N(x)\quad\text{(position)}, \tag{13}$$

$$p_n=D_n(x)\,\frac{dN(x)}{dx}\quad\text{(momentum)}, \tag{14}$$

$$m=1\quad\text{(inertia)}, \tag{15}$$

$$K=-i\omega\quad\text{(spring constant)}. \tag{16}$$

Here, the PHO Hamiltonian is a constant of the motion[11] and assumes the meaning of the total generalized energy E of the plasma wave field, with the PHO angular spatial frequency

$$\Omega_n\equiv\sqrt{K/m}=\sqrt{\omega}e^{-i\pi/4}. \tag{17}$$

Letting from Eq. (11)

$$\alpha(0)\equiv\alpha_0=\left(D_n(0)\,\frac{1+i\omega\tau(0)}{i\omega\tau(0)}\right)^{1/4}N(0), \tag{18}$$

as well as

$$p_n(0)\equiv p_{n0}, \tag{19}$$

after some mathematical calculations it can be shown that

$$\alpha(\zeta)=\frac{p_{n0}e^{i\pi/4}}{\sqrt{\omega}}\sinh[H_n(x)]+\alpha_0\cosh[H_n(x)] \tag{20}$$

and

$$p_n(\zeta)=p_{n0}\cosh[H_n(x)]+\sqrt{\omega}e^{i\pi/4}\alpha_0\sinh[H_n(x)], \tag{21}$$

where

$$H_n(x)\equiv\int_0^x\sigma_n(y,\omega)dy \tag{22}$$

and $\sigma_n(x,\omega)$ is the magnitude of the depth-dependent complex plasma-wave vector[9] defined as

$$\sigma_n^2(x,\omega)\equiv\frac{1+i\omega\tau(x)}{D_n(x)\tau(x)}. \tag{23}$$

Physically, the structure of the carrier plasma wave number $\sigma_n(x,\omega)$ evolves (i) from an ''instantaneously'' formed (i.e., within time $\Delta t\ll\omega^{-1}$[11]), free-carrier spatial distribution, which at low modulation frequencies $f\ll 1/2\pi\tau(x)$ is in-phase with the photoexcitation modulation source and otherwise independent of modulation frequency to (ii) a wavelike, frequency-dependent character of the propagating carrier spatial distribution, as f increases, so that $f\geqslant 1/2\pi\tau(x)$, (iii) when $f\gg 1/2\pi\tau(x)$ the wave field becomes pseudopropagating. In fact, it is highly localized within a diffusion length from the photoexcitation source position, owing to the efficient spatial decay of the oscillation, with behavior identical to conventional diffusion-wave fields, such as thermal-wave oscillations.[12]

Equations (20) and (21) yield a generalization of the well-known $(p(t)=mdx(t)/dt)$ momentum coordinate

$$p_n(\zeta)=\sqrt{\omega}e^{-i\pi/4}\frac{d\alpha(\zeta)}{d\zeta}. \tag{24}$$

B. Free carrier density in an electronically inhomogeneous semiconductor

Substituting Eq. (20) for $\alpha(\zeta)$ in Eq. (13), expanding the hyperbolic terms, and taking into account the boundary conditions, Eqs. (3) and (4), yields the following expression for the plasma density distribution:

$$N(x)=\frac{N_0\sqrt{Q(x)}}{\sigma_n(0)D_n(0)+s\eta}\left(\frac{1-e^{-2[H_n(\infty)-H_n(x)]}}{1+e^{-2H_n(\infty)}}\right)e^{-H_n(x)}, \tag{25}$$

where

$$Q(x)\equiv\frac{D_n(0)\sigma_n(0)}{D_n(x)\sigma_n(x)} \tag{26}$$

and

$$\eta\equiv\frac{1-e^{-2H_n(\infty)}}{1+e^{-2H_n(\infty)}}. \tag{27}$$

On formulating Eq. (25) the generalized carrier-density spatial derivative $dF(x)/dx|_{x=0}$ of the function

$$F(x)\equiv\frac{1}{2}\left(\frac{i\omega\tau(x)}{D_n(x)[1+i\omega\tau(x)]}\right)^{1/4} \tag{28}$$

was neglected. The validity of this (only) approximation to the theory is discussed in the Appendix. It can be easily seen that in the special case where τ and D_n are depth independent, $H_n(\infty)\to\infty$ and Eq. (25) yield the simple expression

$$N(x)=\frac{N_0}{\sigma_nD_n+s}e^{-\sigma_nx}, \tag{29}$$

which is precisely the result obtained for a homogeneous semi-infinite semiconductor with strong surface absorption.[2,8,13]

To satisfy specific physical requirements, let the total plasma-wave field be a linear superposition of three fields:

$$N(x,\omega)=aN_{\text{inh}}(x,\omega)+bN_{0h}(x,\omega)+cN_{\infty h}(x,\omega), \tag{30}$$

where (a,b,c) are arbitrary constants; $N_{\text{inh}}(x,\omega)$ represents the contribution of the inhomogeneous medium, and $N_{0h}(x,\omega)$, $N_{\infty h}(x,\omega)$ are the homogeneous fields with τ and D_n values equal to those at surface and infinity, respectively,

$$N_{0h}(x,\omega)=\frac{N_0}{\sigma_{n0}D_{n0}+s}e^{-\sigma_{n0}x}, \tag{31}$$

$$N_{\infty h}(x,\omega)=\frac{N_0}{\sigma_{n\infty}D_{n\infty}+s}e^{-\sigma_{n\infty}x}, \tag{32}$$

where by definition $\sigma_n(0)\equiv\sigma_{n0}$, $\sigma_n(\infty)\equiv\sigma_{n\infty}$, $D_n(0)\equiv D_{n0}$, and $D_n(\infty)\equiv D_{n\infty}$.

These two homogeneous fields are related to the total plasma-wave field through the following evident limits:

$$\lim_{x\to\infty}N(x,\omega)=N_{\infty h}(x,\omega), \tag{33}$$

$$\lim_{\omega\to\infty}N(0,\omega)=N_{0h}(0,\omega), \tag{34}$$

$$\lim_{\omega\to 0}N(0,\omega)=N_{\infty h}(0,\omega). \tag{35}$$

Taking the indicated limits, the three arbitrary constants of Eq. (30) can be fixed uniquely, using Eqs. (25), (31), and (32). After some algebra one finds the final general expression for the frequency dependence of the plasma density at the surface of an electronically inhomogeneous semi-infinite semiconductor:

$$N(0,\omega)=N_{0h}(0,\omega)[1+(R_{n\infty}-1)e^{-(P_{n\infty}(\omega)-P_{n\infty}(0))}], \tag{36}$$

where

$$R_{n\infty}\equiv\frac{D_{n0}\sigma_{n0}+s}{D_{n\infty}\sigma_{n\infty}+s} \tag{37}$$

and

$$P_{n\infty}(\omega)\equiv\lim_{x\to\infty}[\sigma_{n\infty}x-H_n(x)], \tag{38}$$

with the requirement

$$\lim_{\omega\to\infty}P_{n\infty}(\omega)=\infty. \tag{38'}$$

N_{0h} is defined by Eq. (31).

The physical origin of the $P_{n\infty}(0)$ term in Eq. (36) is due to the fact that at low modulation frequencies $\omega\tau(x)\ll 1$ the plasma density loses its wavelike properties[9] and becomes independent of the modulation frequency with a plasma diffusion length given by Eq. (23):

$$L_n(0)\equiv\sigma_n^{-1}(0)\approx\sqrt{D_n(x)\tau(x)} \tag{39}$$

so that $P_{n\infty}(0)\neq 0$.

From the foregoing formalism and the generality of $D_n(x)$ and $\tau(x)$ profiles assumed in the PHO field, it is clear that the generalized Hamilton–Jacobi theory of the free-carrier transport dynamics in harmonically photoexcited semiconductors can handle arbitrary depth distributions of these parameters. Specifically, Eq. (36) is valid for increasing, decreasing, and nonmonotonic $\tau(x)$ and/or $D_n(x)$ depth profiles.

C. A special case: Exponential profiles

In order to see phenomenologically how the (so far arbitrary) inhomogeneities of electronic transport properties influence the plasma density frequency dependence it is convenient to assume some specific depth profiles for $\tau(x)$ and $D_n(x)$ and calculate $P_{n\infty}(\omega)$, Eq. (38). As an example, the following monotonically increasing or decreasing exponential dependencies will be discussed based on the simple physical rule that the amount of damage caused at a given depth in a semiconductor through, e.g., ion implantation, is proportional to the density of the damage-causing agent (ions) at that depth. A square dependence of the exponential function will be further assumed for convenience,[14] so that the integration in Eq. (22) may give analytic results. The effect of the square dependence is essentially negligible compared to the strong exponential character of the functions under consideration:

$$\tau(x)=\tau_\infty(1\pm\Delta e^{-qx})^2,\quad \Delta=\left|\sqrt{\frac{\tau_0}{\tau_\infty}}-1\right|, \tag{40}$$

and

$$D_n(x)=D_{n\infty}(1\pm\delta e^{-qx})^2,\quad \delta=\left|\sqrt{\frac{D_{n0}}{D_{n\infty}}}-1\right|, \tag{41}$$

where the positive and negative signs are related to decreasing and increasing depth profiles, respectively. Here (τ_0, D_{n0}) and (τ_∞, $D_{n\infty}$) characterize the semiconductor surface and bulk transport parameters, respectively. In what follows, for independently variable transport parameters, several different combinations of the above profiles will be considered; they may correspond to different semiconductor samples and/or experimental conditions.

1. Constant τ, variable $D_n(x)$

In this simplest case, when $\tau_\infty=\tau_0\equiv\tau$ upon calculating the integral in $H_n(x)$, Eq. (22), and the limit in Eq. (38), one finds for both increasing and decreasing $D_n(x)$ profiles of Eq. (41):

$$P_{n\infty}(\omega)-P_{n\infty}(0)=\frac{1}{2q}\,L_{n\infty}^{-1}\left|\ln\left(\frac{D_{n0}}{D_{n\infty}}\right)\right|(\sqrt{1+i\omega\tau}-1), \tag{42}$$

where $L_{n\infty}=\sqrt{D_{n\infty}\tau}$ is the plasma diffusion length in the bulk. It is easy to verify that the condition Eq. (38′) is satisfied.

Correspondingly, the $R_{n\infty}$ coefficient, Eq. (37), becomes

$$R_{n\infty}=\left(\frac{D_{n0}\sqrt{1+i\omega\tau}+sL_{n0}}{D_{n\infty}\sqrt{1+i\omega\tau}+sL_{n\infty}}\right)\frac{L_{n\infty}}{L_{n0}}, \tag{43}$$

and the final expression for the carrier density at the surface is obtained by substituting Eqs. (42) and (43) into Eq. (36).

2. Constant D_n, variable $\tau(x)$

Using the same procedure as above and taking both the increasing and decreasing $\tau(x)$ profiles as described by Eq. (40), gives

$$P_{n\infty}(\omega)=\pm\frac{1}{q}\sqrt{\frac{i\omega}{D_n}}\,(\sqrt{1+B^2}\,\ln(G_1)+B\,\ln(G_2)-\ln(G_3)), \tag{44}$$

where the positive and negative signs are related to decreasing and increasing $\tau(x)$ profiles, respectively, and the following definitions have been made:

$$G_1\equiv\frac{1}{2}\left(\frac{|\Delta-1|+B^2}{1+B^2}+\sqrt{\frac{(\Delta-1)^2+B^2}{1+B^2}}\right), \tag{45}$$

$$G_2\equiv\frac{B+\sqrt{1+B^2}}{B+\sqrt{(\Delta-1)^2+B^2}}\,|\Delta-1|, \tag{46}$$

$$G_3\equiv\frac{\sqrt{(\Delta-1)^2+B^2}-|\Delta-1|}{\sqrt{1+B^2}-1}, \tag{47}$$

and

$$B\equiv(i\omega\tau_\infty)^{-1/2}. \tag{48}$$

For $P_{n\infty}(0)$ and $R_{n\infty}$ one finds

$$P_{n\infty}(0)=\frac{1}{2q}\,L_{n\infty}^{-1}\left|\ln\left(\frac{\tau_0}{\tau_\infty}\right)\right|, \tag{49}$$

and

$$R_{n\infty}=\left(\frac{D_n\sqrt{1+i\omega\tau_0}+sL_{n0}}{D_n\sqrt{1+i\omega\tau_\infty}+sL_{n\infty}}\right)\frac{L_{n\infty}}{L_{n0}}, \tag{50}$$

where $L_{n\infty}$ and L_{n0} are now equal to $\sqrt{D_n\tau_\infty}$ and $\sqrt{D_n\tau_0}$, respectively.

3. Variable $\tau(x)$ and $D_n(x)$

In this general case, when both the carrier lifetime and diffusivity are depth dependent, with the same gradient (as expected from surface-treated materials), we obtain

$$P_{n\infty}(\omega)=\pm\frac{1}{q}\sqrt{\frac{i\omega}{D_{n\infty}}}\,[\sqrt{1+B^2}\,\ln(G_1)+(1+\mu)B\,\ln(G_2)-\sqrt{1+\mu^2B^2}\,\ln(G_4)], \tag{51}$$

where the following definitions were made:

$$G_4 \equiv \frac{\sqrt{(\Delta-1)^2+B^2}\sqrt{1+\mu^2B^2}+B^2\mu-|\Delta-1|}{\sqrt{1+B^2}\sqrt{1+\mu^2B^2}+B^2\mu-1} \times|\delta-1|^{-1}, \tag{52}$$

and

$$\mu \equiv \frac{\delta}{\Delta-\delta}, \quad \Delta \neq \delta. \tag{53}$$

For $P_{n\infty}(0)$ and $R_{n\infty}$ one can find

$$P_{n\infty}(0)=\frac{1}{2q}L_{n\infty}^{-1}\left[(1+\mu)\left|\ln\left(\frac{\tau_0}{\tau_\infty}\right)\right|+\mu\left|\ln\left(\frac{D_{n0}}{D_{n\infty}}\right)\right|\right]. \tag{54}$$

and

$$R_{n\infty}=\left(\frac{D_{n0}\sqrt{1+i\omega\tau_0}+sL_{n0}}{D_{n\infty}\sqrt{1+i\omega\tau_\infty}+sL_{n\infty}}\right)\frac{L_{n\infty}}{L_{n0}}, \tag{55}$$

where $L_{n\infty}=\sqrt{D_{n\infty}\tau_\infty}$ and $L_{n0}=\sqrt{D_{n0}\tau_0}$.

It is easy to verify that in the case of depth-independent carrier diffusivity Eq. (51) is reduced to Eq. (44). On the other hand, assuming only the $D_n(x)$ profile in Eqs. (51) and (54), one can obtain Eq. (42), as expected. As before, condition Eq. (38′) is satisfied for both Eq. (44) and Eq. (51).

It can be shown that Eq. (51) (with some modification of signs) is very flexible and is still valid for opposing profiles, e.g., decreasing $\tau(x)$ and increasing $D_n(x)$ or vice versa, which are mostly of theoretical interest and will not be discussed further.

In conclusion, the special case Eqs. (51)–(54), together with the general Eq. (36), and profiles, Eq. (40) and Eq. (41), are the key formulas of the present work: they describe generally possible experimental situations, and can be used for carrier dynamic studies in inhomogeneous semiconductors with particular $\tau(x)$ and $D_n(x)$ profiles. In practice, Eq. (36) can be linked to a suitable photothermal diagnostic methodology, which is known to be sensitive to free carrier densities. In this manner, specific or arbitrary depth profiles of $\tau(x), D_n(x)$ may be reconstructed in what amounts to the inverse problem.

III. SIMULATIONS OF THE GENERALIZED THEORY

In the following simulations of the carrier dynamics in inhomogeneous semiconductors, increasing electronic diffusivity and/or lifetime profiles will be assumed, corresponding to the physical situation where the semiconductor sample surface is modified (damaged) and the values of the electronic parameters there are lower than those of the unaltered bulk.

Following the theoretical model of Sec. II, variable $D_n(x)$ and $\tau(x)$ profiles will be examined separately, as well as together: it turns out that diffusivity and lifetime inhomogeneities influence the surface plasma density (SPD) magnitude and phase frequency behavior in different ways.

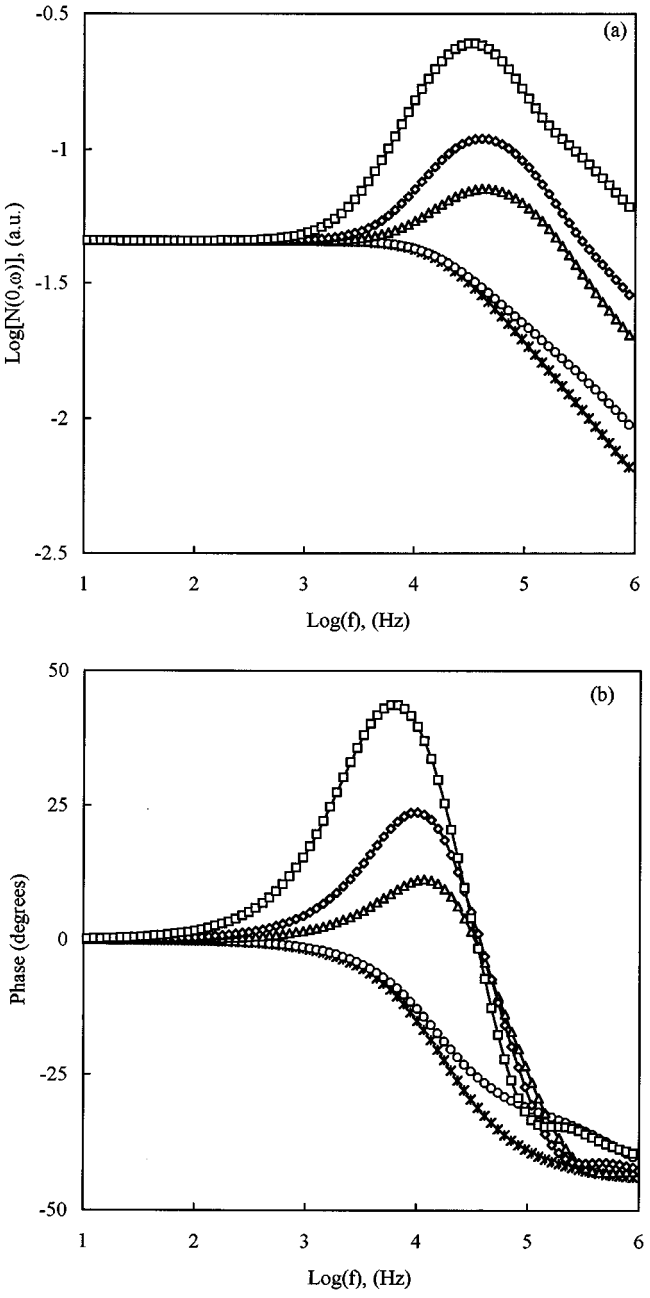

FIG. 1. Effect of the surface carrier diffusivity (D_{n0}) on the SPD magnitude (a) and phase (b) frequency responses for a semiconductor with depth-dependent carrier diffusivity $D_n(x)$: D_{n0}=0.1 (□), 0.5 (◇), 1.0 (△), 5.0 (○), and 10.0 (*) cm^2/s. Parameters used for calculation: $D_{n\infty}$=10 cm^2/s, τ=10 μs, q=10^4 m^{-1}, s=100 cm/s.

A. Depth-dependent carrier diffusivity

Figure 1 shows the effect of the surface carrier diffusion coefficient D_{n0} on the frequency response of a semiconducting sample with an exponentially increasing profile $D_n(x)$, Eq. (41), and constant minority carrier lifetime. It can be seen that an increase in the degree of inhomogeneity, manifested by the steepening of the gradient between the D_{n0} and $D_{n\infty}$ values, results in increasing the SPD magnitude at high frequencies with respect to its flat value at low frequencies [Fig. 1(a)]. The corresponding phase dependence also exhibits this positive deviation from its zero values at low frequen-

cies [Fig. 1(b)]. At low frequencies both magnitude and phase are flat as expected from the frequency in dependence of the plasma-wave vector, Eq. (23). In the limit of $\omega \rightarrow \infty$ the slope of the SPD magnitude frequency response becomes that of a homogeneous sample with phase saturated at $-45°$ and electronic properties those of the material surface. The effect of the surface electronic diffusivity value appears in the peak amplitude and position: for lower D_{n0} this peak is more pronounced owing to the steeper $\partial D_n(x)/\partial x$ gradient, and shifted toward the low frequency edge for both magnitude and phase (Fig. 1). The curve behaves in the conventional manner[2] when $D_{n0}=D_{n\infty}$, i.e., with zero gradient.

The effect of changing surface recombination velocity on the SPD magnitude and phase frequency response is somewhat similar to that produced by D_{n0} (Fig. 1). An increasing s reduces the positive peak amplitude and shifts it toward high frequencies. In addition, high surface recombination decreases the plasma density in the bulk, thus resulting in the depression of the flat SPD magnitude levels at low frequencies. However, for low s values below a critical recombination velocity, the effect of the surface recombination is very weak and can be neglected. From Eqs. (31) and (43) the low frequency condition $s \ll \sqrt{D_{n0}/\tau}$ can be established, which gives $s \ll 340$ cm/s as the critical recombination velocity for the choice of calculation parameters in Fig. 1 and $D_{n0}=1$ cm^2/s.

The effect of the diffusivity profile steepness constant q is illustrated in Fig. 2. At high modulation frequencies, i.e., near the sample surface, both the SPD magnitude and phase frequency behavior are that of a homogeneous sample with $D_n=D_{n0}$. Correspondingly, at low frequencies the magnitude and phase are frequency independent at a level of a homogeneous sample with $D_n=D_{n\infty}$. The steeper the diffusivity profile (higher q), the more confined to the near-surface region the perturbation in the electronic transport properties of the sample, resulting in higher peak probe frequencies for the shallower subsurface inhomogeneity (Fig. 2). Secondary oscillations for the deepest profile ($q=10^3$ m^{-1}) can also be observed; these are associated with effective plasma reflections and peak frequency determined by the plasma-wave wavelength becoming commensurate with the thickness of the effective surface layer. The diffusivity gradient separates the sample into two virtual layers with diffusion coefficient values D_{n0} (surface thin layer) and $D_{n\infty}$ (substrate). Thinner effective-diffusivity layers corresponding to larger q values exhibit higher peak reflection frequencies, owing to the reduced plasma wavelength. These oscillations are imperceptible in the amplitude plots, Fig. 2(a), but can be gleaned in the phase plots, Fig. 2(b), in the range 0.1–1 MHz.

Summarizing the above results, it is concluded that both SPD magnitude and phase are sensitive to the inhomogeneities introduced by spatially varying carrier diffusivity and that they exhibit a relative signal enhancement with characteristic positive peaks whose amplitudes and positions generally depend on the surface diffusivity value and profile steepness.

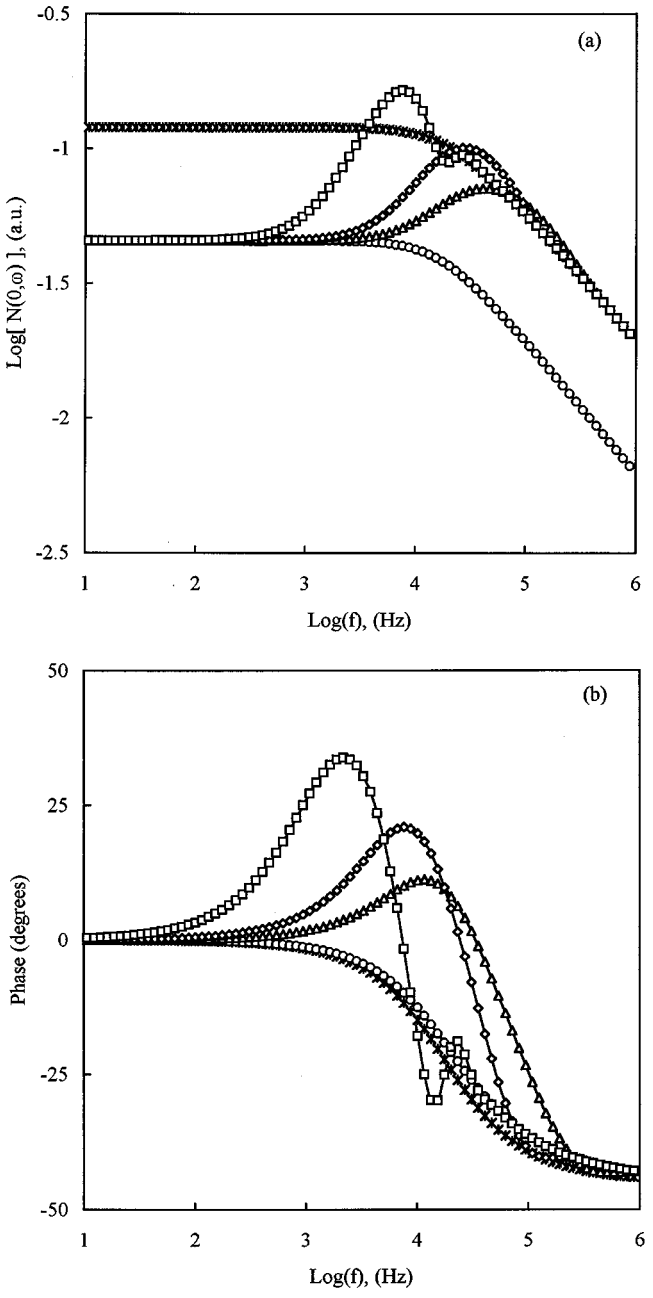

FIG. 2. Effect of the steepness constant (q) of the carrier diffusivity profile on the SPD magnitude (a) and phase (b) frequency responses for a semiconductor with depth-dependent carrier diffusivity $D_n(x)$: $q=10^3$ (□), 5×10^3 (◇), and 10^4 (△) m^{-1}. $D_{n0}=1$ cm^2/s, other parameters are the same as in Fig. 1. Two other lines represent a homogeneous sample with $D_n=1$ cm^2/s (○) and $D_n=10$ cm^2/s (∗), respectively.

B. Depth-dependent carrier lifetime

In contrast to the variable diffusivity case, inhomogeneities introduced by a spatially varying carrier lifetime result in a clear, sharp negative peak in the SPD magnitude frequency response [Fig. 3(a)] and large phase perturbations [Fig. 3(b)]. This negative magnitude peak appears in the frequency range where $\omega\tau \sim 1$, while at low and high modulation frequencies the SPD magnitude dependencies are equivalent to those of a homogeneous sample. This feature is a manifestation of the smooth transition of the model to the

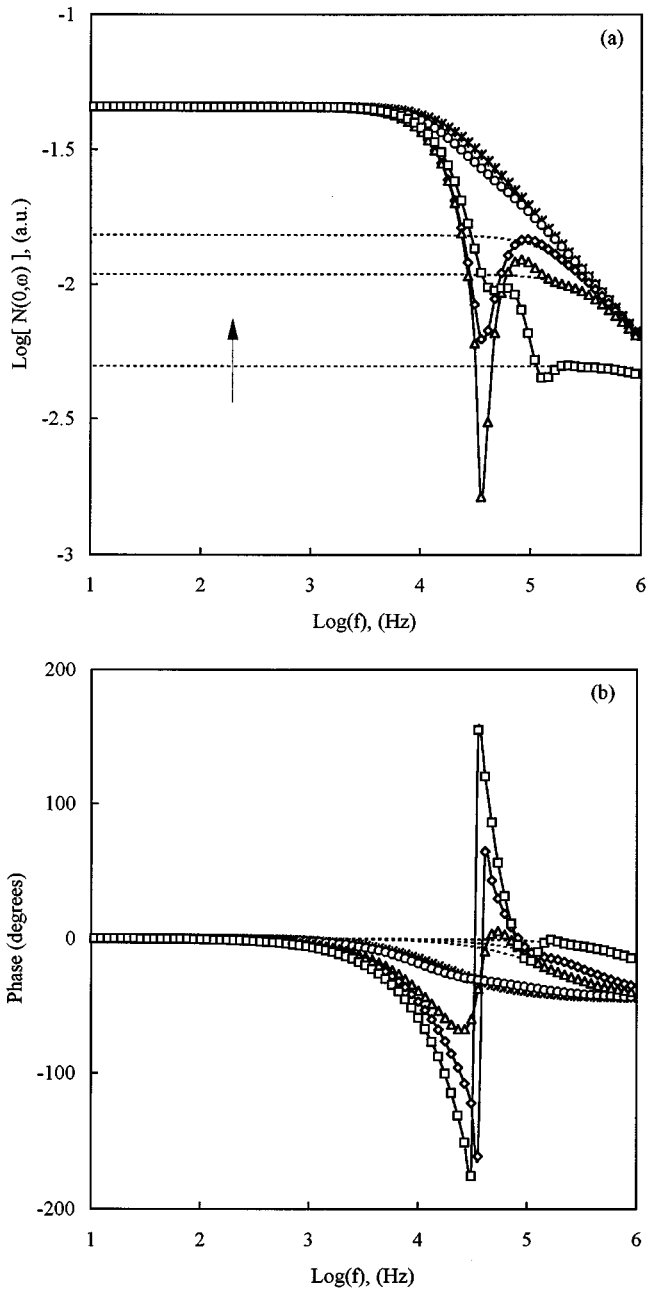

FIG. 3. Effect of the surface carrier lifetime (τ_0) on the SPD magnitude (a) and phase (b) frequency responses for a semiconductor with depth-dependent carrier lifetime $\tau(x)$: τ_0=0.1 (□), 0.5 (◇), 1.0 (△), 5.0 (○), and 10.0 (*) μs. Parameters used for calculation: τ_∞=10 μs, D_n=10 cm^2/s, q=10^4 m^{-1}, s=100 cm/s. The dotted lines in the direction shown in (a) represent a homogeneous sample with τ=0.1, 0.5, and 1.0 μs, respectively.

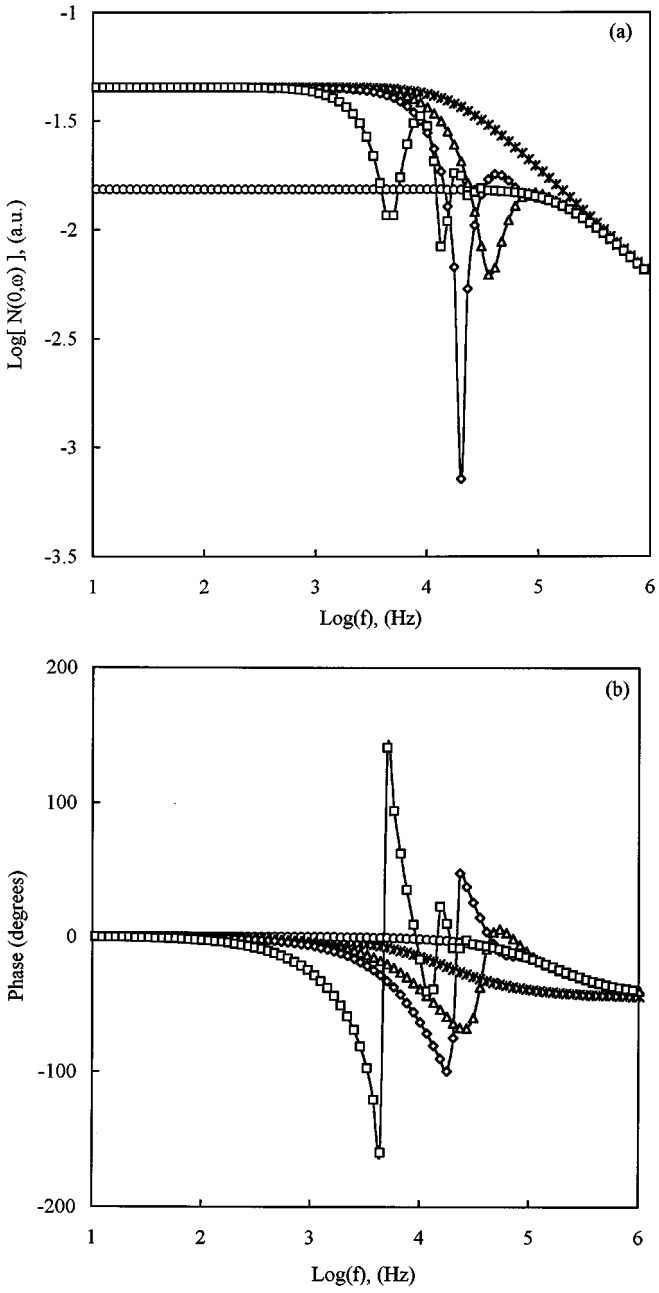

FIG. 4. Effect of the steepness constant (q) of the carrier lifetime profile on the SPD magnitude (a) and phase (b) frequency responses for a semiconductor with depth-dependent carrier lifetime $\tau(x)$: q=10^3 (□), 5×10^3 (◇), and 10^4 (△) m^{-1} s=100 cm/s, τ_0=1 μs; other calculation parameters are the same as in Fig. 3. The two remaining lines represent a homogeneous sample with τ=10 μs (*) and τ=1 μs (○), respectively.

homogeneous cases with $\tau=\tau_\infty$ and $\tau=\tau_0$ at the respective frequency limits. The amplitude of the inverted peak depends strongly on the gradient of the surface lifetime. The peak disappears when the sample is nearly homogeneous [Fig. 3(a)]. The associated phase frequency response shows significant variations that reach ~320° at the steepest gradient (τ_0=0.1 μs).

The effect of increasing the surface recombination velocity in this case appears as a depression in magnitude and a strong phase oscillation, similar to those observed in Fig. 3. However, contrary to the diffusivity case, an increase in s does not change the positions of the peaks, which are determined by the lifetime gradient $\partial\tau(x)/\partial x$.

Finally, the gradient of the lifetime profile affects the SPD magnitude and phase frequency dependencies nearly in the same manner as with variable diffusivity: a decrease in q shifts the magnitude peak position to lower frequency and makes it more pronounced [Fig. 4(a)]. It can be noted that for a changing $\tau(x)$ gradient there is a ''critical'' profile (indeed, a combination of varying parameters) when the negative

peak reaches its maximum value. Below this value the SPD magnitude frequency behavior becomes more complicated, partly because of plasma-wave reflections across the width of the layer with variable lifetime. In a manner similar to Fig. 2, the extrema due to plasma reflections appear at higher frequencies with increasing q, i.e., with the narrowing of the inhomogeneous near-surface layer. Overall, both the SPD magnitude and phase are very sensitive to τ_0 and the profile gradient, as described by the q parameter.

It is interesting to note that the foregoing characteristic features of the SPD magnitude and phase frequency responses caused by an inhomogeneous lifetime, i.e., the sharp negative peak and strong phase perturbations, are quite similar to several features observed earlier in a number of studies on the competition between the contributions from the thermal and electronic components of the temperature gradient in, what were thought to be, homogeneous semiconductors.[5,8,15,16]

C. Simultaneous depth profiles in carrier diffusivity and lifetime

In this general case the SPD magnitude and phase frequency responses are a complex superposition of contributions from carrier diffusivity and lifetime inhomogeneities and have a dominant lifetimelike character. It can be shown that *only* for high frequencies *and/or* high profile gradient parameter (q) does the combined diffusivity-lifetime term, Eq. (51), become the simple linear superposition of the ''pure'' diffusivity and lifetime terms, Eqs. (42)–(44), so that both the total magnitude and phase curves can be obtained by an addition of the corresponding dependencies. The effect of D_n and τ spatial gradients in this case is also similar to that for the lifetime profiles. As expected, both magnitude and phase are more sensitive to the lifetime spatial variations than to those of the carrier diffusivity.

IV. COMPARISON WITH TWO-LAYER MODEL AND EXPERIMENTAL RESULTS

The present generalized inhomogeneous plasma propagation theory was compared with the limiting discrete case of the two-layer sample model developed by Opsal and Rosencwaig (OR).[9,10] For convenience, the $M(\omega)$ ratio of the surface plasma density for the inhomogeneous sample to that for a homogeneous one was used. The results are presented in Fig. 5. It can be seen that for very steep diffusivity and lifetime profiles and a thin layer assumed for the OR model calculation, the *trends* in both magnitude and phase frequency are in reasonable agreement. However, for both depth-dependent diffusivity and lifetime the actual discrepancies between the two theories are significant. Figure 5 indicates that, in the limit where the thin inhomogeneous surface layer is much narrower than the plasma wavelength, the inhomogeneous region behaves almost like a discrete homogeneous layer on a homogeneous substrate. It is also shown that the present model has the necessary frequency resolution to diagnose near-surface inhomogeneities in experimental data.

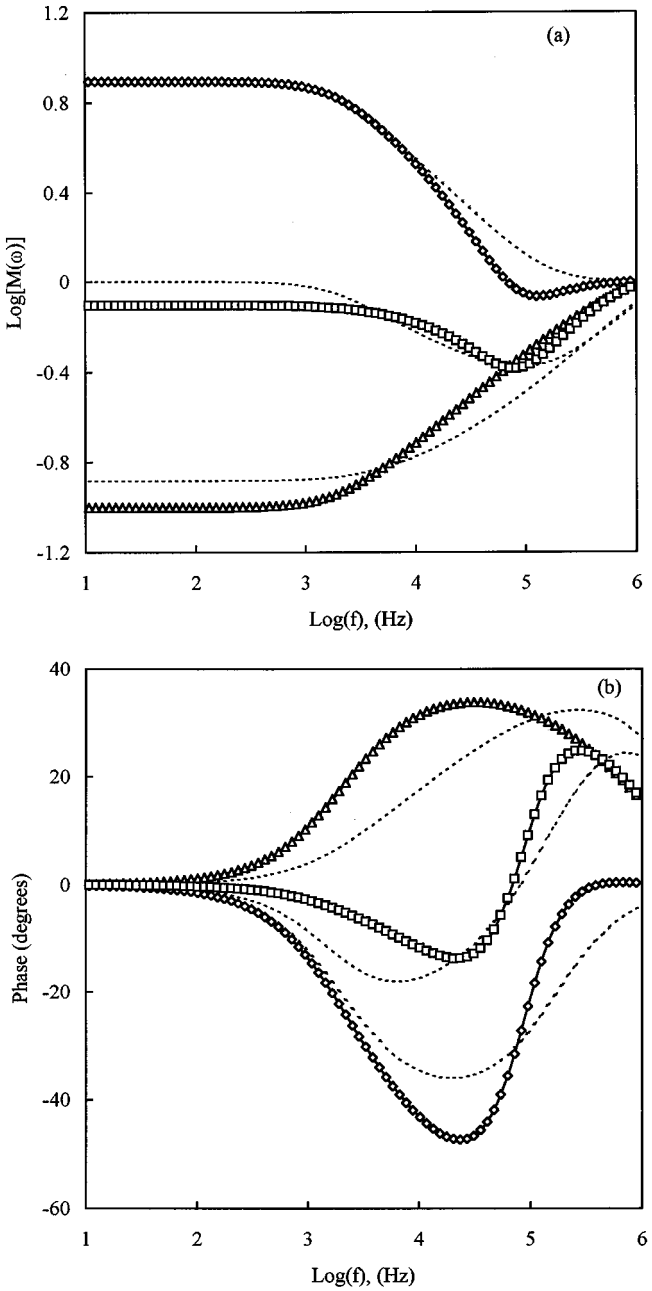

FIG. 5. The $M(\omega)$ ratio of inhomogeneous to homogeneous sample magnitude (a) and phase (b) frequency response calculated by using the present model (symbols) and the two-layer model of Opsal and Rosencwaig (OR) (Refs. 9 and 10) (dotted lines): (△) inhomogeneous carrier diffusivity only: $D_{n0}=0.1$ cm^2/s, $D_{n\infty}=9$ cm^2/s, $\tau=100$ μs; (◇) inhomogeneous carrier lifetime only: $\tau_0=1$ μs, $\tau_\infty=100$ μs, $D_n=9$ cm^2/s; (□) both inhomogeneous diffusivity and lifetime: $D_{n0}=0.1$ cm^2/s, $D_{n\infty}=9$ cm^2/s, $\tau_0=1$ μs, $\tau_\infty=100$ μs. Parameters used for the calculation: $s=100$ cm/s, $q=10^5$ m^{-1}. OR model: layer thickness $d=1$ μm and subscripts ''0'' and ''∞'' are assigned to the surface layer and bulk parameters, respectively.

The model was applied to preliminary experimental results obtained by using the PTR detection technique with a Si sample implanted with P^+ ions of 50 keV energy to the dose of 10^{12} cm^{-2} (Fig. 6). The photothermal signal from the nonimplanted (homogeneous) part of the same Si wafer was used to calculate $M(\omega)$. In this preliminary study the main interest is in the shape of the $M(\omega)$ ratio magnitude and

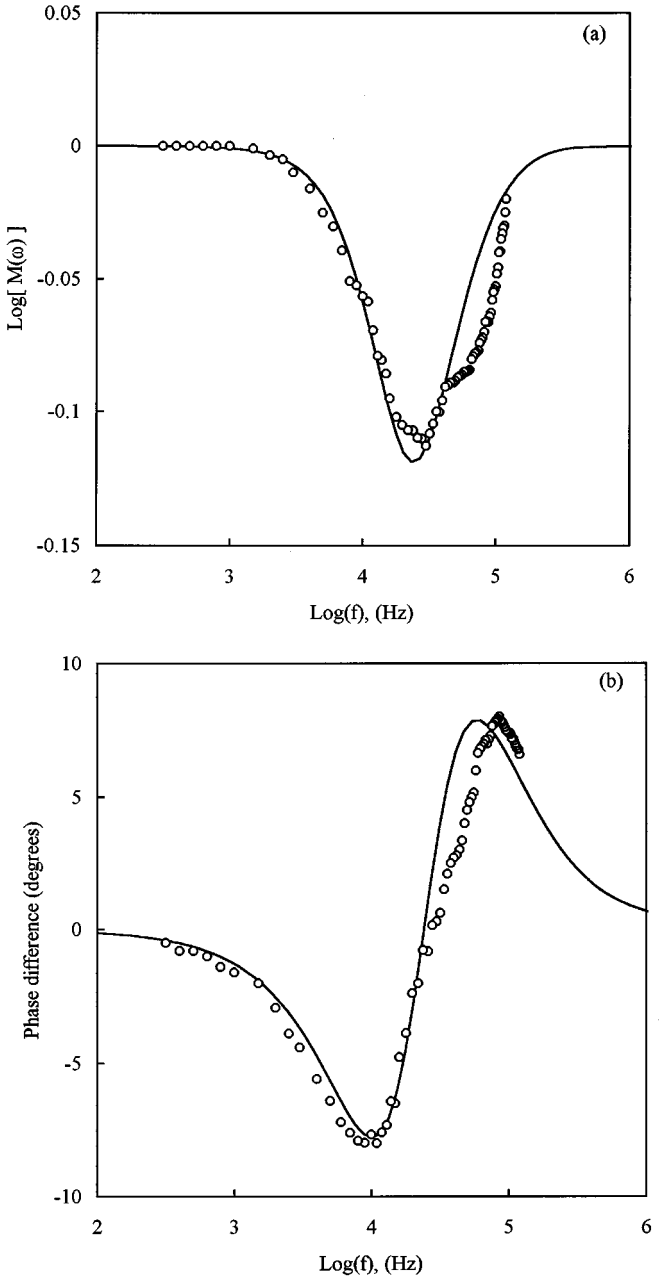

FIG. 6. Comparison of the $M(\omega)$ ratio of experimental amplitudes (a) and phase difference (b) frequency responses for a P^+-implanted Si sample (circles) and theoretical simulations (solid lines) using the following parameters: $D_n=20$ cm^2/s, $\tau_0=5$ μs, $\tau_\infty=15$ μs, $s=300$ cm/s, $q=5\times10^4$ m^{-1}.

phase frequency responses, since actual depth profiles are not expected to be purely exponential. A comparison of characteristic features—negative peak in magnitude and phase behavior—with the theoretical predictions, concluded that they are due to increasing lifetime inhomogeneities with small variations in D_n. Fitting of the experimental results by the theoretical model yielded an increasing exponential lifetime profile with parameters shown in the caption of Fig. 6 and possible D_n changes ranging between 15 and 25 cm^2/s. The middle value $D_n=20$ cm^2/s has been used in the fitting program (Fig. 6). Despite the simple exponential profile simulation, the experimental results and the theoretical simulations are in very good agreement for both the magnitude and phase, thus largely justifying the simple physical rule assumption leading to Eqs. (40) and (41).

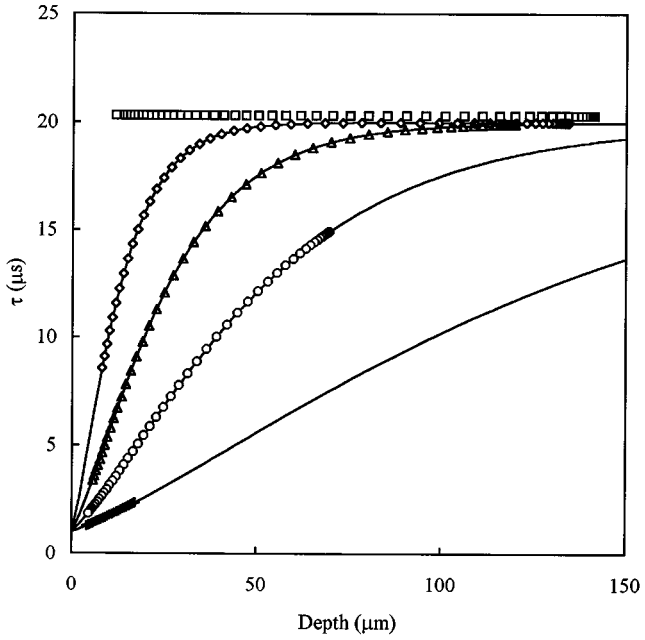

FIG. 7. Assumed (lines) and reconstructed (points) carrier lifetime exponential profiles of different steepnesses: homogeneous sample (□), $q=1000$ (◇), 500 (△), 250 (○), and 100 cm^{-1} (*). Parameters used: $D_n=10$ cm^2/s, $\tau_0=1$ μs, $\tau_\infty=20$ μs, $s=100$ cm/s.

V. THE PLASMA-WAVE INVERSE PROBLEM

Finally, using the experimental results of Fig. 6, the lifetime profile for the P^+-implanted Si sample has been reconstructed. The two-dimensional Broyden's method was used[17] which searches for the surface values τ_0 and q satisfying the minimum conditions both in $M(\omega)$ ratio's magnitude (M) and phase ($\Delta\phi$) simultaneously:

$$|M_{\exp}(\omega_i)|-|M_{\text{theor}}(\omega_i)|=0, \tag{56}$$

$$|\Delta\varphi_{\exp}(\omega_i)|-|\Delta\varphi_{\text{theor}}(\omega_i)|=0, \tag{57}$$

for each modulation frequency ω_i.

The basic feature of plasma-wave depth profiling via consideration of the inverse problem, which makes it quite different from the same procedure in the thermal-wave case,[14,18] is that $\tau(x)$ and $D_n(x)$ profiles can be reconstructed only partially. Due to the peculiar frequency behavior of the a/c plasma diffusion length $L_n\equiv\sigma_n^{-1}$, Eq. (23), which is frequency independent when $\omega\tau(x)\ll1$ and lifetime independent when $\omega\tau(x)\gg1$, for each $\tau(x)$ and/or $D_n(x)$ profile there is a limited depth range within which these profiles can be reconstructed (Fig. 7). This range depends on both surface and bulk values, profile steepness, and modulation frequency range. As can be seen from Fig. 7, even for the homogeneous sample the lifetime profile can be reconstructed within the depth range 12–140 μm for the 10 Hz–1 MHz modulation frequency range used in this example.

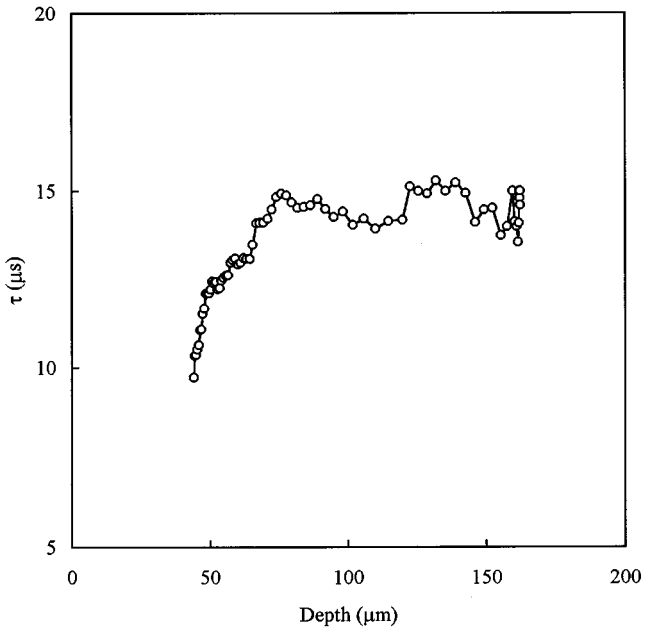

FIG. 8. Results of the reconstruction of the carrier lifetime profile from the magnitude and phase frequency data of Fig. 6.

The results of the two-dimensional search, Eqs. (56) and (57), are presented in Fig. 8. The inversion uses the (q and τ_0) pair as unknown variables to fit the magnitude and phase data at each frequency and is capable, in principle, of reconstructing *arbitrary* profiles. The effective $\tau(x)$ profile reconstruction depth range appeared to be 44–162 μm for the given D_n value (20 cm^2/s) that was assumed constant in the searching program. At low frequencies, i.e., probing the material bulk, the lifetime is found to be nearly constant at the 15 μs level which is in good agreement with the known value for a nonimplanted Si sample.[19] Here the plasma wave is independent of modulation frequency ($\omega_{\min}\tau_\infty \ll 1$) and the reconstruction depth is limited by the plasma diffusion length $L_n \approx 175$ μm. At high frequencies, i.e., close to the damaged surface, the lifetime decreases reaching the value of 10 μs at the lowest available depth $x_{\min}=42$ μm. The reconstruction depth limit here is due to the lifetime-independent L_n at high frequencies, Eq. (39), when $\omega_{\max}\tau_0 \gg 1$. It can be shown that the lifetime profiles reconstructed assuming different (but close) values of D_n are similar to those presented in Fig. 8.

As a result of the solution to the plasma-wave inverse problem, it was found that the implantation process introduces structural electronically sensitive defects in the Si sample spread much deeper than the nominal thickness of the implanted layer itself.

VI. CONCLUSIONS

The generalized Hamilton–Jacobi plasma-wave theory of a continuously inhomogeneous semiconductor with arbitrary $\tau(x)$ and $D_n(x)$ depth profiles was developed. Carrier plasma-wave amplitude and phase frequency behavior simulations using the developed general theoretical model with specific, physically motivated exponential lifetime and electronic diffusivity depth profiles clearly show the high sensitivity of a frequency scan to spatial changes both in carrier diffusivity *and* lifetime. These theoretical predictions are in very good agreement with preliminary experimental data from a surface-modified (ion-implanted) semiconductor Si sample. They allow one to distinguish between the dominant contributions from diffusivity and/or lifetime inhomogeneities and evaluate the nature and extent of damage penetration through its effect on the surface and bulk electronic parameters, profile type, and steepness.

The general results of the forward path of the depth-profiling problem were further used to address the inverse problem. The reconstruction of computer simulated depth profiles of the carrier lifetime was performed and excellent results were obtained. The first experimental lifetime profile reconstruction was also performed using the two-dimensional Broyden method for the inverse path on amplitude and phase data from a moderately implanted Si wafer probed with infrared photothermal radiometry. Deep implantation effects on the lifetime that induced a decrease of more that 50% near the wafer surface from the value of the bulk lifetime were observed. The foregoing inverse algorithm forms a basis for further constructing improved signal inversion methodologies. The use of higher modulation frequencies in the range where the signal becomes independent of lifetime will allow the inversion of very shallow electronic diffusivity depth profiles. Experimental and theoretical studies of these problems are currently in progress.

ACKNOWLEDGMENTS

The authors wish to gratefully acknowledge the support of the Natural Sciences and Engineering Research Council of Canada (NSERC) for a Collaborative Research Grant. One of the authors (A.S.) is also grateful to NSERC for a NATO Science Research Fellowship Award.

APPENDIX: CRITIQUE OF THE ONLY MATHEMATICAL APPROXIMATION TO THE THEORY

The only approximation in the formulation of the theoretical development leading to the key equations, Eqs. (36) and (51)–(54), was the assumption that the derivative of Eq. (28) can be neglected in the formulation of the generalized carrier density field $N(x)$, Eq. (25):

$$F_x(0) \equiv \left.\frac{dF(x)}{dx}\right|_{x=0} \approx 0. \tag{A1}$$

Actually, the assumption, Eq. (A1), states that the contribution to the plasma density profile from a term proportional to the spatial rate of change of the inverse square root of the product $D_n(x)\sigma_n(x)$ is negligible. If that term is included in the calculation of the plasma density flux at the surface [applying the boundary condition, Eq. (3), to $N(x)$ in the form of Eq. (25)], an extra term will appear:

$$D_n(0)\left(F(0)\sigma_n(0)\frac{P_{n0}}{\sqrt{i\omega}} + f_x(0)\alpha_0 \right) = -N_0 + s\alpha_0 F(0). \tag{A2}$$

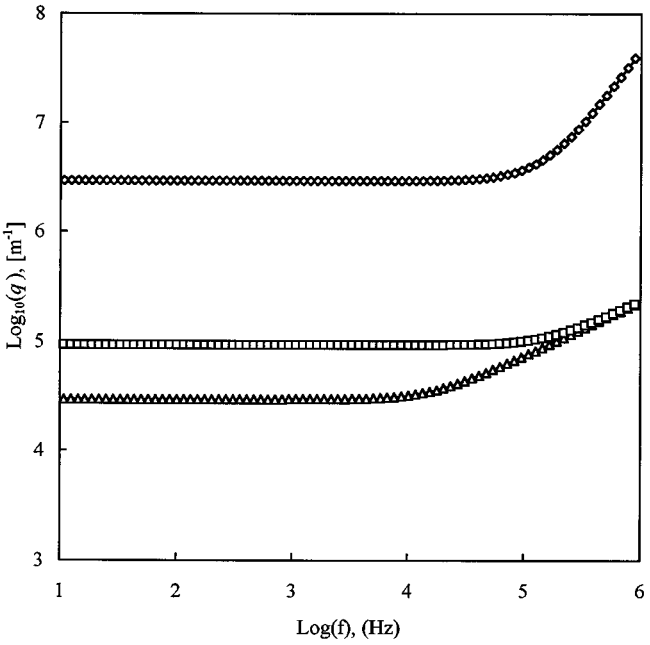

FIG. 9. Plot of the conditions (A4)–(A6) as equations of q vs modulation frequency for ($\diamond$) depth-dependent carrier lifetime only ($\tau_0=1$ μs, $\tau_\infty=10$ μs, $D_n=10$ cm^2/s); ($\square$) both depth-dependent lifetime and diffusivity ($D_{n0}=1$ cm^2/s, $D_{n\infty}=10$ cm^2/s, $\tau_0=1$ μs, $\tau_\infty=10$ μs, and ($\triangle$) depth-dependent carrier diffusivity only ($D_{n0}=1$ cm^2/s, $D_{n\infty}=10$ cm^2/s, $\tau=10$ μs).

Using the boundary conditions, Eqs. (3) and (4), expressions for α_0, p_{n0} may be determined and it can be shown that the above term will be negligible if and only if

$$|F(0)\sigma_n(0)| \gg |f_x(0)|. \tag{A3}$$

It is easy to verify that, upon taking the indicated derivative, relation (A3) amounts to ascertaining that

$$q|L_{n\infty}-L_{n0}| \ll 2(1+\omega^2\tau^2)^{1/4}, \tag{A4}$$

for $D_n(x)$ profiles [Eq. (41), case in Sec. II C1], or

$$q|L_{n\infty}-L_{n0}| \ll 2(1+\omega^2\tau_0^2)^{3/4}\left(\frac{\tau_\infty}{\tau_0}\right)^2, \tag{A5}$$

for $\tau(x)$ profiles [Eq. (40), case in Sec. II C2], and

$$qL_{n0}\left[\left(\sqrt{\frac{\tau_\infty}{\tau_0}}-1\right)\left(\frac{\tau_0}{\tau_\infty}\right)^2-\left(\sqrt{\frac{D_{n\infty}}{D_{n0}}}-1\right)(1+\omega^2\tau_0^2)^{1/2}\right] \ll 2(1+\omega^2\tau_0^2)^{3/4}, \tag{A6}$$

for $\tau(x)$ and $D_n(x)$ profiles [Eqs. (40) and (41), general case in Sec. II C3], where $L_{n\infty}$, L_{n0} keep their original definition for each case. As expected, the condition for the general case, Eq. (A6), gives the two other conditions, Eqs. (A4) and (A5), when constant lifetime or diffusivity, respectively, is assumed.

For all profiles considered in Sec. III for the simulation of the carrier wave amplitude and phase frequency behavior, conditions (A4)–(A6) were found to be satisfied within the frequency range used.

As an example, the above inequalities were solved for q and plotted as equations in Fig. 9, versus modulation frequency for three different profiles with the values of surface and bulk lifetimes and diffusivities indicated. It can be easily seen that the values of q used for the simulations in Sec. III are much smaller than those calculated in Fig. 9, thus satisfying the inequalities, Eqs. (A4)–(A6).

[1] A. Rosencwaig, in *Photoacoustic and Thermal-Wave Phenomena in Semiconductors*, edited by A. Mandelis (Elsevier, New York, 1987), Chap. 5.
[2] J. Sheard, M. G. Somekh, and T. Hiller, Mater. Sci. Eng. B **5**, 101 (1990).
[3] T. M. Hiller, M. G. Somekh, S. J. Sheard, and D. R. Newcombe, Mater. Sci. Eng. B **5**, 107 (1990).
[4] Z. H. Chen, R. Bleiss, A. Mandelis, A. Buczkowski, and F. Shimura, J. Appl. Phys. **73**, 5043 (1993).
[5] A. Skumanich, D. Fournier, A. C. Boccara, and N. M. Amer, Appl. Phys. Lett. **47**, 402 (1985).
[6] J. Pelzl, D. Fournier, and A. C. Boccara, in Vol. 69, *Springer Series in Optical Sciences*, edited by D. Bicanic (Springer, Berlin, 1987), p. 241.
[7] A. Rosencwaig, J. Opsal, W. L. Smith, and D. L. Willenborg, Appl. Phys. Lett. **46**, 1013 (1985).
[8] A. C. Boccara and D. Fournier, in Ref. 1, Chap. 12.
[9] J. Opsal and A. Rosencwaig, Appl. Phys. Lett. **47**, 498 (1985).
[10] J. Opsal and A. Rosencwaig, J. Appl. Phys. **53**, 4240 (1982).
[11] H. Goldstein, *Classical Mechanics* (Addison-Wesley, Reading, MA, 1965), Chap. 9.
[12] A. Mandelis, J. Math. Phys. **26**, 2676 (1985).
[13] N. Mikoshiba, H. Nakamura, and K. Tsubouchi, Proceedings of the IEEE Ultrasonic Symposium, 1982, p. 580.
[14] A. Mandelis, S. B. Peralta, and J. Thoen, J. Appl. Phys. **70**, 1761 (1985).
[15] A. O. Salnick, Ph.D. thesis, Moscow Physics Engineering Institute, Moscow, 1991.
[16] D. Fournier, A. C. Boccara, A. Skumanich, and N. M. Amer, J. Appl. Phys. **59**, 787 (1986).
[17] F. Funak, A. Mandelis, and M. Munidasa, J. Phys. (France) III **4**, C7 (1994).
[18] A. Mandelis, E. Schoubs, S. B. Peralta, and J. Thoen, J. Appl. Phys. **70**, 1771 (1991).
[19] R. E. Wagner, Ph.D. thesis, University of Toronto, Toronto, 1994.